SYSTEM DESIGN FOR ENHANCED *IN SITU* MONITORING OF IONIZING RADIATION EFFECTS IN SEMICONDUCTOR DEVICES

Chee Fuei Pien, Haider F. Abdul Amir & Saafie Salleh

School of Science and Technology
Universiti Malaysia Sabah, 88999 Kota Kinabalu, Sabah, Malaysia

ABSTRACT. *The amount of ionizing radiation that semiconductor devices encounter during their lifecycle degrades both of their functional and electrical parameter performances. Different radiation environments either in space, high energy physics experiments, nuclear environment or fabrication process as well as for standard terrestrial operation possess an impact on the device. The development in the semiconductor industry, however, is not driven predominantly with space applications or radiation hardness alternatives. Hence, there is a need to access the effects of ionizing radiation on semiconductor devices. This designed system offers the ability to access the changes in the properties of the semiconductor devices when being irradiated by integrating in situ method. This is to identify the hardness of the semiconductor devices under test to be used within a range of ionizing radiation environment and to evaluate their operating region under radiation environments. This system developed provides a better accuracy in term of data acquiring and it is different from the conventional methods that the changes in electric characteristics of the devices are analyzed at post-irradiations.*

KEYWORDS. Ionizing, hardness, *in situ*, post-irradiations

INTRODUCTION

Interaction of semiconductor devices with energetic ionizing photons (gamma rays and x-rays) leads to the mechanism of ionization damage (Messenger & Ash, 1992). This damage arises due to the following interactions: photoelectric effect, Compton Effect and pair production depending on the photon energy, E_{PH} (Najim, 2009). Therefore, the semiconductor device that exposed to an ionizing radiation environment typically endures degradation in one or more on its performance parameters.

At the low energy extreme for x-rays which is of the order of a few keV, the interactions are mainly through photoelectric effect that a photon is absorbed by an atom and one of the atomic electrons, photoelectron is released (Krane, 1988). The photoelectric effect that undergoes in semiconductor devices causes a bonding valence electron to be emitted into the conduction band across the band gap, E_g, leaving behind a hole. This yields the creation of a free electron-hole pair.

For higher energy photons, the main interaction with matter is due to the Compton Effect. Compton Scattering occurs when the incident photon is deflected from its original path due to the interaction with an electron that is free or relatively bound to an atom (Messenger & Ash, 1992). In this interaction, the photon loses energy as part of the photon energy is transferred to the electron which in turn yields the emitting of a secondary lower energy photon. If the energy is above the threshold, this photon can again be absorbed to create a second electron-hole (E-H) pair. Hence, an average number of E_{PH}/E_{EH} carrier pairs will be generated in the semiconductor material, which is proportional to the original photon energy (Claeys & Simoen, 2002).

As for very high energy photons, the interaction that most probably occurs is the pair production. Pair production is the formation of an electron and a positron from sufficiently energetic photon traveling through matter, usually in the vicinity of an atomic nucleus without violating the conservation of momentum (Heyde, 1999). The energy is conserved in this interaction that the kinetic energies of the moving electron and positron with their equivalent mass (*m*), $E=mc^2$ add up to the energy supplied by the initiating photon (Lowenthal & Airey, 2001). The atomic nucleus as the third interacting particle in this interaction is necessary in conserving the momentum.

The Linear Energy Transfer (LET) function, $\rho m^{-1} \frac{dE}{dx}$ is used to determine the total energy deposited in the semiconductor material through ionizing interactions (Claeys & Simoen, 2002). In this function, ρm represents the density of the material interacted, E is the radiation energy whereas dx is an elementary trajectory in the material.

This paper explores the feasibility and accuracy of integrating in situ method in a data acquiring (DAQ) system. This comes along with the objective of placing this system into a processing tool to obtain real time measurement of changes in the selected semiconductor devices induced by radiation.

SUMMARY OF SYSTEM DESIGNED FEATURES

A. Overview

This data acquisition system developed is comprised of three parts; an I/O hardware (driver circuit), a host computer and the controlling software. The in situ operation occurs without interrupting the normal state of this system and it is the key element in monitoring the local conditions of an operating device in radiation environment.

This applied technique has numerous advantages such as increased measurement speed, reduced sensor introduction cost, and increased spatial and temporal resolution. This application also produces a high accuracy system as it improved the process monitoring; reduce product variance and higher throughput.

B. Hardware Physical Model

The data acquiring hardware will be based on two ways interface which are the analog to digital converter (ADC) and digital to analog converter (DAC).

Analog to digital conversion is used in this system to compare a series of trial analog signals to the analog signal to be measured until two signals match within a specific tolerance. The analog signal will then be converted to digital format, which can be interpreted by the host computer. The code width of this 16-bit ADC with a full scale voltage of 10V is approximately 0.1526 mV. Therefore, a very small change occur in the devices during irradiation is reliable to be detected.

The method of analog to digital conversion used in this system is Voltage to Frequency Converter (VFC). VFC is a generator which the output frequency is proportional to an input voltage. The construction of the VFC is as shown in Figure 1. This VFC contains two stage operational amplifiers (Op amp) and a precision pulse generator (NE555). The first stage Op amp is configured as a Miller Integrator together with an R-C network whereas the second stage Op amp is operated as a comparator.

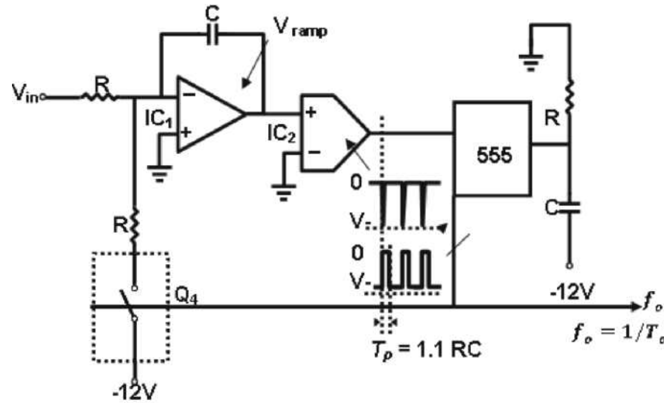

Figure 1. The Construction of Voltage to Frequency ADC.

The integrator action of the first stage Op amp arises from the combination of high negative gain, *A* of the amplifier and an increase in the equivalent input capacitance that appears across the Op amp input terminals. This increase in the input capacitance is given by

$$C = (1 + A)\,\Delta C \tag{1}$$

where ΔC is the feedback capacitance.

The Miller effect will then affect the input impedance and the frequency response of the amplifier. The signal outputted from the first stage Op amp consists of excessive rounding in both of the rising edge and the falling edge of the signal during the charging and discharging process of the R-C network. Hence, the signal will be fed to the second stage Op amp which configured as a comparator in order to sample and interpret the signal.

The analog input V_{IN-} of the comparator is grounded (0V) which is configured as the reference voltage, V_{REF}. Hence when the signal applied to the analog input V_{IN+} of the comparator is greater than the V_{IN-} (0V), the output of the comparator will produce a digital high level (logic 1). When the analog input at V_{IN+} is less than the analog input V_{IN-}, the output of the comparator is a digital low level (logic 0). The signal is inverted by the 555 timer circuit which is configured as monostable mode in order to obtain a lower duty pulses as shown in Figure 1.

This process repeats continuously, producing a digital pulse-train at the VFC output. The output waveform of the VFC is as shown in Figure 2. As the input voltage increases, the time constant, *t* will increase which in turn cause a rise in the frequency.

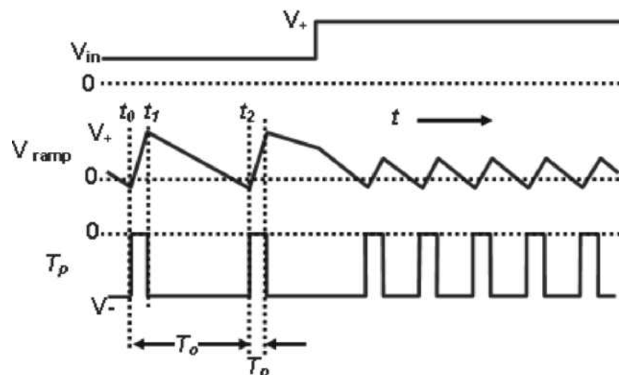

Figure 2. The output waveform of the VFC.

The 4 bit DAC implemented performs the transformation from the digital domain to the analog domain. This DAC takes digital inputs and generate an analog voltage or current as output to control the device under test (DUT) by receiving commands from the host computer. The output generated by this DAC will be remained until it receives another value from the computer. The block diagram of microprocessor digital to analog converter interface is as shown in Figure 3. Consequently, the measuring hardware is equipped with timing circuitry to produce a pulse train of a constant frequency to control the ADC and DAC.

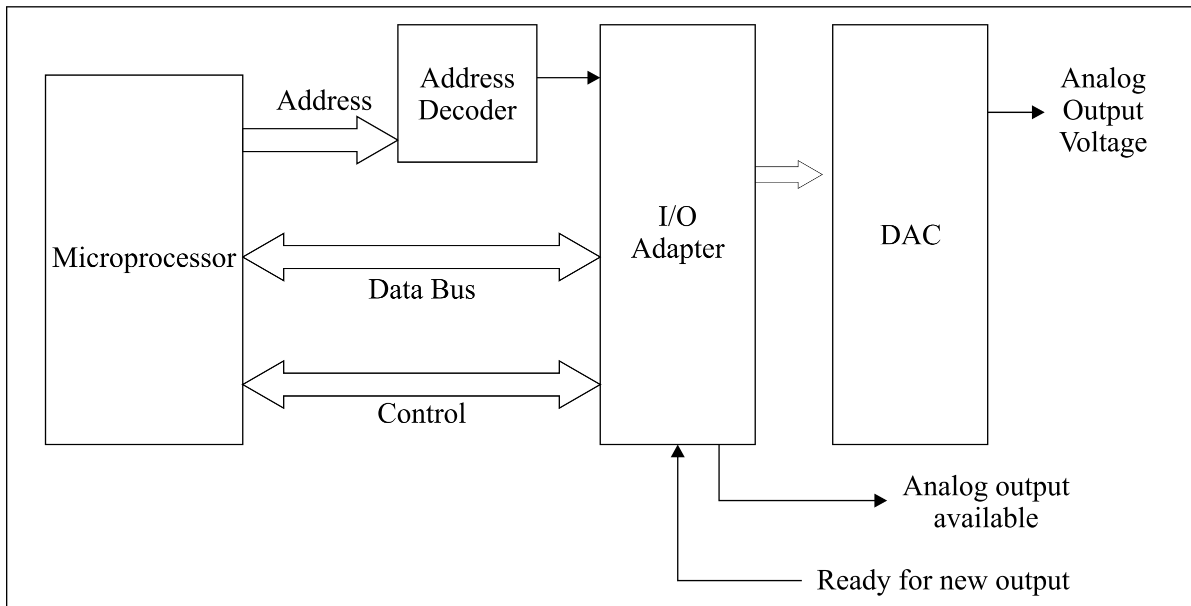

Figure 3. Block diagram of microprocessor digital to analog converter interface.

The ADC and DAC interfaces are collectively known as semiconductor device driver circuit. This peripheral driver circuit is integrated by an I/O serial adapter to the microprocessor. This I/O adapter is selected by sending out its address on the address bus and then using control signals to write or read from the driver circuit.

C. Software Development and Graphical User Interfaces

The software is developed using Visual Basic programming language. It consisted of programming codes running under the DOS and Windows operating system. The process flow of the main software developed is as shown in Figure 4.

The functionality of the software can be divided into two parts EXE application files. The first part serves as the asynchronous protocol in the serial communications between the hardware and software. The Graphical User Interface (GUI), namely Serial Port Configuration is as shown in Figure 5. It is designed mainly to detect the address of the I/O serial adapter that integrated the driver circuit and for some basic configuration settings of communication.

A Start Conversion (SC) signal is generated when the correct address transmitted by the microprocessor activates the I/O adapter. At the end of the conversion, the ADC sends signals to the control circuit that the conversion is over and that the data can be read. This is indicated by the End Of Conversion (EOC) signal. This serial transmission between the driver circuit and I/O serial adapter is as shown in the Figure 6.

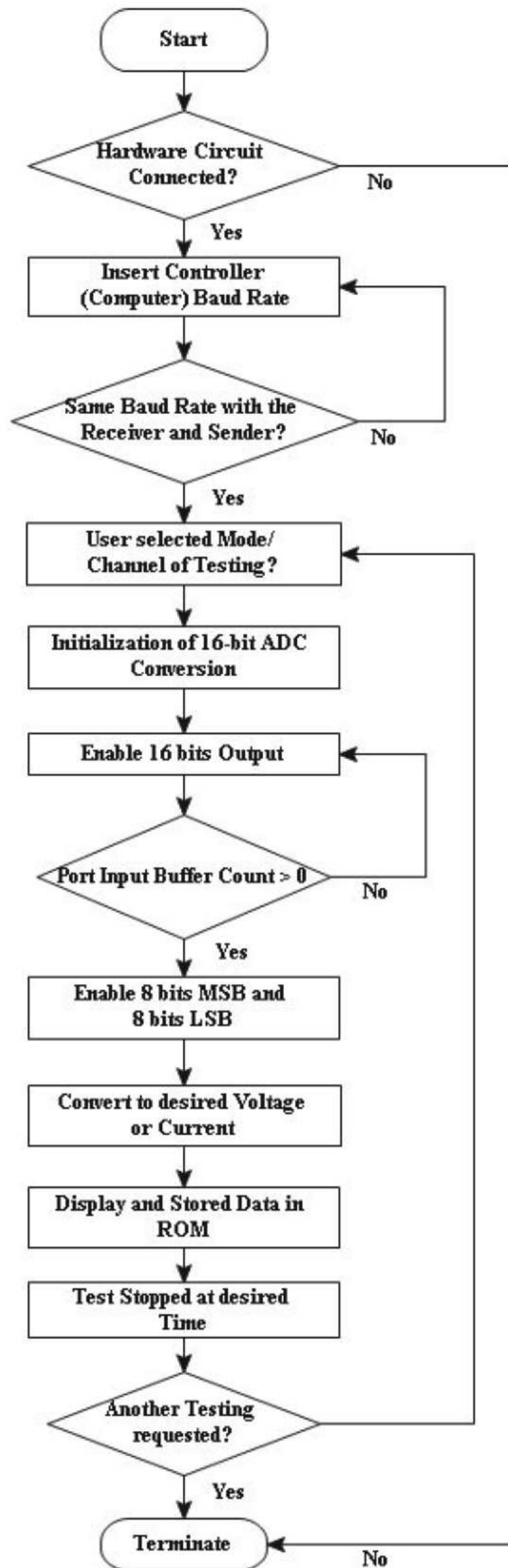

Figure 4. The flowchart of the developed software.

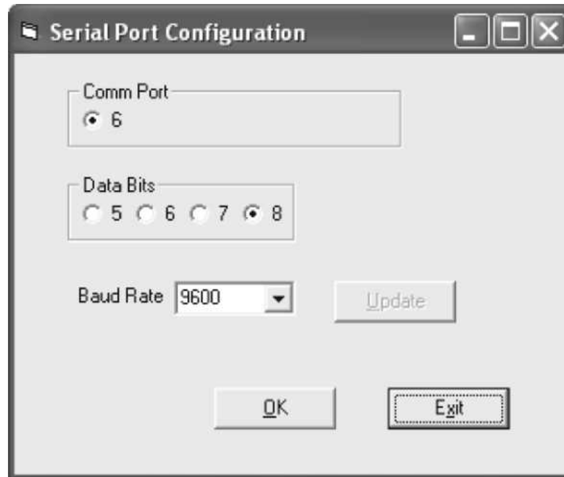

Figure 5. The GUI of the Serial Port Configuration

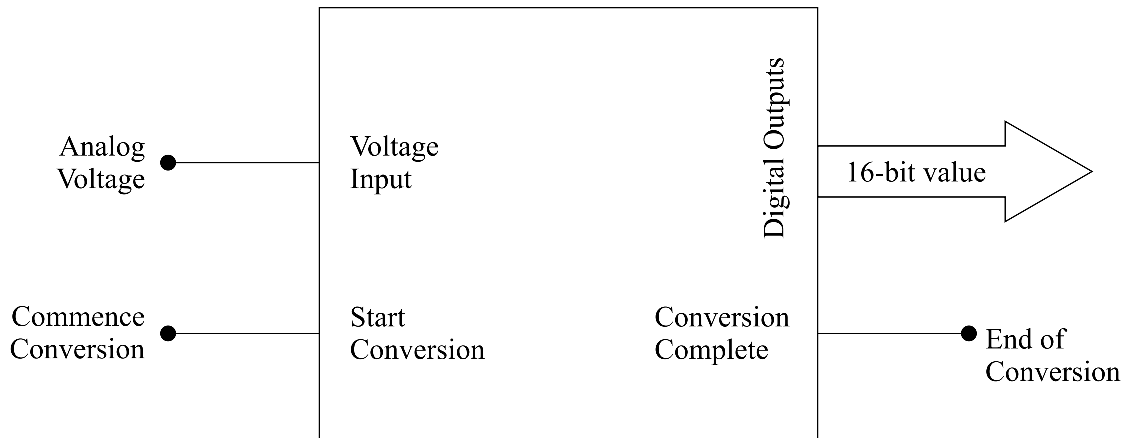

Figure 6. Block Diagram of the Serial Transmission between the Control Circuit and the I/O Adapter.

The second part of the software is used to monitor the changes in parameter of the devices under test (DUT). The GUI of the application, namely Software Interface is as shown in Figure 7. This EXE application file performs the following functions:

(a) Processing the input digital signals, including arithmetical operations, comparison, ordering, and code conversion,
(b) Display in numerical form,
(c) Transmission,
(d) Storage for further data handling, and
(e) Changing the characteristics (current and voltage) of the devices under test (DUT).

Figure 7. The GUI of the Software Interface

RADIATION TEST PROCEDURE

Exposures are conducted with gamma ray sources, Cobalt-60 (Co-60) source on optoelectronic devices. The water is transferred into irradiation chamber through matrix pumps by means of piston pump. This process is computerized and operated by hydraulic system. The water is then allowed to flow continuously throughout matrix pipes which placed in a special configuration, whereby Co-60 will be situated in between matrix pipes upon lifting up from underground. This special configuration control the distance between the optoelectronic devices under test and Co-60 source, allowing equal exposure of radiation.

The input voltage of the particular device can be varied from a distance of approximately 15m in a control room during irradiation and the effect can be observed directly using *in situ* method. The schematic drawing of the test setup for in situ testing is shown in Figure 8. The information and status of the devices under test (DUT) will be transmitted through the driver circuit based on an ADC circuit into the PC. Cables used to connect this system should never be led to any serious distortion of the shape of signals or the degradation of reliability in data communication. The temperature dependence of the charge deposition in the sampling device will be monitored with an electronic thermometer using LM35 precision centigrade temperature sensor.

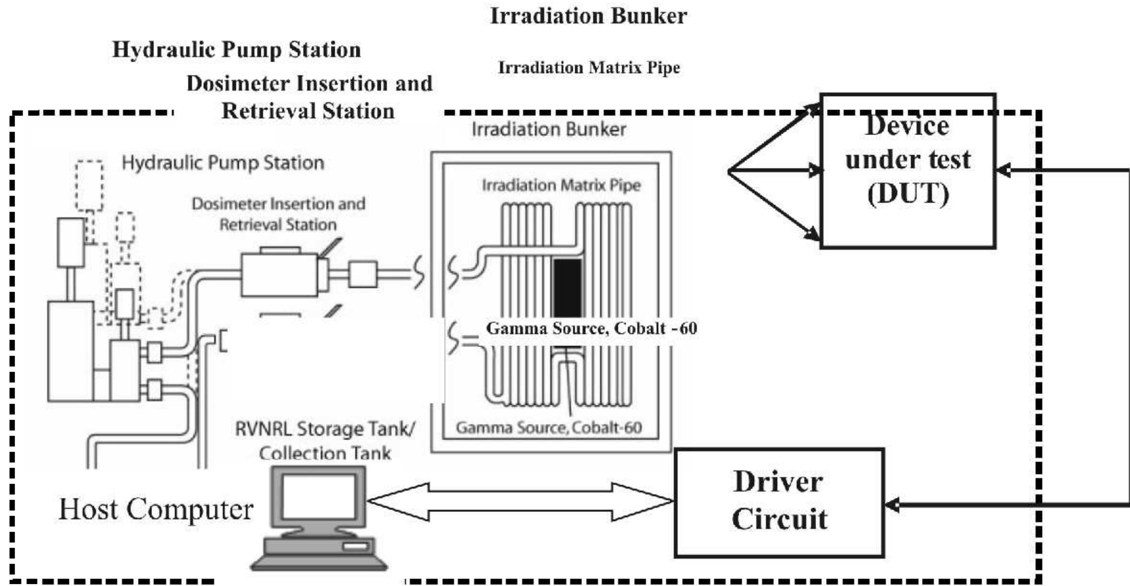

Figure 8. Co-60 Irradiation Test Setup

The ionizing radiation releases high energy charged particles in almost every material. When these reactions take place near the sensitive region of the DUT, electric charges induced by the ionization effect of the high energy particles will change the bias voltage of the sampling device. However, these changes are not permanent and are recoverable with the control signals from the PC.

The optoelectronic devices used in this test consisted of a Plastic Infrared Light Emitting Diode (QEE 113) coupled to a Plastic Silicon Infrared Phototransistor (QSE 113). The phototransistor eventually acts as a reference sensor in this test. The Setup of the devices is as shown in Figure 9.

Electrical measurements are performed *in situ* by connecting this setup of DUT to the driver circuit board built via a double shielded cable. This board serves as the power supply to the DUT. Moreover, it also acts as a measuring tool to real time monitor the changes in the output power of the reference phototransistor at various dose levels and distances of photo coupling with the input light current I_F as a changing parameter.

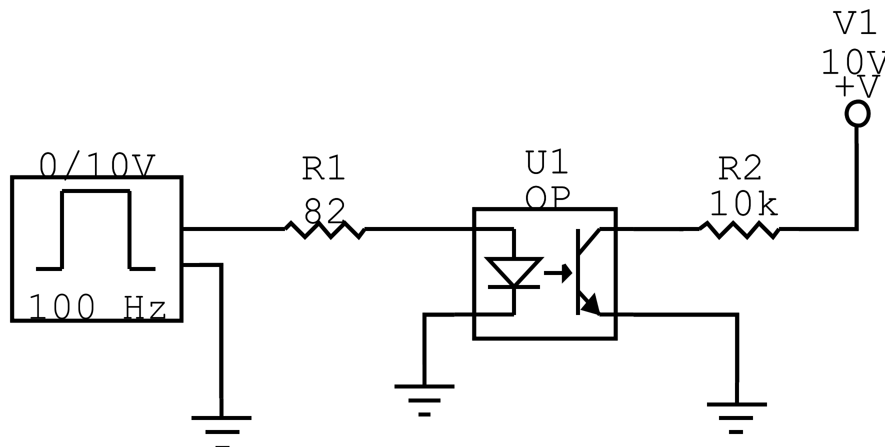

Figure 9. Schematic of Experimental Setup for Optocoupler

RESULTS AND DISCUSSION

Figure 10 shows the results obtained for this setup at pre-irradiation under room temperature. It measures the phototransistor's V_{CE} at a selected value of $I_F = 100mA$ for the IR diode.

The *in situ* test was carried out during irradiation for an absorbed dose of 10 krad which take 32 minutes. The *ex situ* test, however, was taken at post-irradiation of 10 krad using another new set of identical optoelectronic devices for 32 minutes. Another set of control experiment is also being run for 32 minutes without radiation and it served as the reference test.

From the results obtained, it is found the V_{CE} is always higher with the existencevof radiation. This occurs in both of the in situ test and *ex situ* test. The results gained showed great variation between the *in situ* test and *ex situ* test where the readings of V_{CE} that obtained during the *in situ* test are continuously lower than that of *ex situ* test. As a result, this system developed is necessary in order to monitor the characteristic of the devices during irradiation in 'ON' condition.

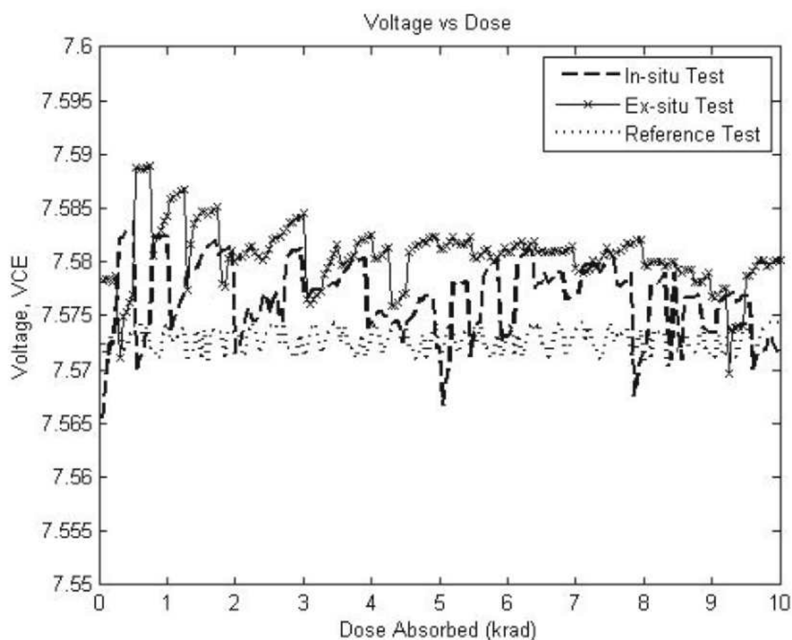

Figure 10. The Phototransistor's V_{CE} at $I_F = 100mA$ for the IR Diode.

CONCLUSIONS

By using the conceptual of *in situ* method applied in this system, the changes in semiconductor devices characteristics are observed and measured directly when the devices are irradiated with gamma ray sources, Cobalt-60 (Co-60).

This implemented data acquisition system also offers a quick method for determining the weak links in an existing system, and an approximation system radiation tolerance at whole. Understanding the mechanism of these damages will be of great help to anticipate the next step of preparation as to strengthen the resistance of these electronics devices against the radiation.

ACKNOWLEDGEMENTS

The authors are thankful to Science Fund 2007, MOSTI, Project No.: SCF0046-STS-2007, with title "Effects of Total Dose Irradiation on Semiconductor Devices".

REFERENCES

Banks, D. 2006. *Microengineering, MEMS, and Interfacing.* Boca Raton: CRC Press, Taylor & Francis Group.

Bisello, D., Candelori, A., Kaminski, A., Litovchenko, A., Noah, E. & Stefanutti, L. 2004. X-ray Radiation Source for Total Dose Radiation Studies. *Journal of ScienceDirect.* **71:**713-715.

Bishop, R.H. 2008. Mechatronic System Control, Logic and data Acquisition (2nd Edition). Boca Raton: CRC Press, Taylor & Francis Group.

Boesch, H. E. Jr., Mclean, F.B., McGarrity, J. M., & Ausman, G. A. Jr. 1978. Hole Transposrt and Charge Relaxayion in Irradiation SiO2 MOS Capacitors. *IEEE Transaction on Nuclear Science.* **22:** 2163.

Fullem, T. Z. 2006. *Radiation detection using single event upsets in memory chips.* New York: State University of New York at Binghamton.

Haider, F. Abdul Amir. 2002. *The Mechanism of MOSFET Damage Induced By Neutron Radiation Resulting from D-T Fusion Reaction.* Ph.D's Dissertation. Gadjah Mada University, Yogyakarta.

Heyde, K. 1999. Basic Ideas and Concepts in Nuclear Physics, 2nd Edition: Institute of Physic Publishing Ltd.

Hurtado, M. 2001. An In situ Method to Measure the Radiation Pattern of a GPS Receiving Antenna. *IEEE Transactions On Instrumentation and Measurement.* **50:** 846-849.

Jassim M. Nakim. 2009. Studying the different Effects of Gamma and X-ray Irradiation on the Electrical Properties of Silicon Diode type 1N1405. *Int. J. Nanoelectronics and Materials.* **2**(1): 41-46.

Johnston, A.H. 2000. Radiation Damage of Electronic and Optoelectronic Devices in Space. *4th International Workshop on Radiation Effects on Semiconductor Devices for Space Application,* October 11-13, 2000, Tsukuba, Japan.

Kouba, C. 1997. *Single Event Effects of the 486-DX4 Microprocessor.* Master's Dissertation. Texas A&M University.

Krane, K.S. 1988. Introductory Nuclear Physics: John Wiley& Sons.

Label, K.A., Kniffin, S. D., Reed, R. A., Kim, H. S., Wert, J. L., Oberg, D. L., Normand, E., Johnston, A.H., Lum, G. K., Koga, R., Crain, S., Schwank, J. R., Hash, G.. L., Buchner, S., Mann, J., Simpkins, L., D'Ordine, M., Marshall, C.A., O'Bryan, M. V., seidleck, C. M., Nguyen, L.X., Carts, M.A., Ladbury, R.L. & Howard, J.W. 2000. A Compendium of Recent Optocoupler Radiation Test Data. 2000 *The IEEE Nuclear and Space Radiation Effects Conference.* Reno, Nevada. 123-146.

Lho, Y. H. & Kim, K. Y. 2005. *Radiation Effects on the Power MOSFET for Space Applications.* ETRI Journal. 27(4): 449-452.

Li, X., Shen, K., Huang, C. M & Chu, L. 2007. A Memory Soft Error Measurement on Production Systems. *2007 USENIX Annual Technical Conference Proceedings.* Santa Clara, CA . 275-280

Lilley, J.S. 2002. Nuclear Physics, Principal and Application.: John Wiley & Sons.

Liu. M. X., han, Z. S., Bi, J. S., Fan, X., Liu, G. & Du, H. 2009. Effect of Total Ionizing Dose Radiation on the 0.25 μm RF PDSOI nMOSFETs with Thin Gate Oxide. *Journal of Semiconductors*. **30**(1): 014004_1-014004_7.

Lowenthal, G.C. & Airey, P.L. 2001. Practical Applications of Radioactivity and Nuclear Radiations.: Cambridge University Press.

Ma, T. P. & Dressendorfer, P. V. 1989. *Ionizing Radiation Effects in MOS Devices & Circuits.* Canada: John Wiley& Sons.

Messenger, G. C. & Ash, M.S.1992. The Effects of Radiation on Electronic System.: Van Nostrand Reinhold.

Parchinskii, P. B. & Ligai, L. G.., Mansurov, Kh. Zh. & Iulchiev, Sh. Kh. 2005. The Effect of γ Radiation on the Temperature Dependence of the Surface Generation Velocity at a Si–SiO_2 Interface. Technical Physics Letters. **31**(4): 288-289.

Park, J. & Mackay, S. 2003. Practical *Data Acquisition for Instrumentation and Control Systems.* Great Britain: Elsevier.

Truscott, P., lei, F., Dyer, C., Ferguson, C., Gurriaran, R., Nieminen, P., daly, E., Apostolakis, J., Giani, S., Pia, M.G., Urban, L. & Maire, M. 2000. Geant4- A New Monte Carlo Toolkit for Simulating Space Radiation Shielding and Effects. *2000 The IEEE Nuclear and Space Radiation Effects Conference.* Reno, Nevada. 147-152.

Tsabaris, C., Bagatelas, C., Dakladas, Th., Papadopoulos, C.T., Vlastou, R. & Chronis, G.T. 2008. An Autonomous *In Situ* Detection System for Radioactivity Measurements in the Marine Environment. *Applied Radiation and Isotopes.* **66:**1419-1426.

Wang, J. & Yang, W. 2008. Effects of Irradiation with Gamma and Beta Rays on Semiconductor Hall Effect Devices. *Journal of ScienceDirect.* **266**(16): 3583-3587.